1 ernational) Conference on Mechanical Engineering-ISME2007
May 15-17, 2007, Amirkabir University of Technology, Tehran, Iran
ISME2007_1981

Equivalent Electrical Simulation of a High -Power Ultrasonic Piezoelectric Transducer by Using Finite Element Analysis

Amir Abdullah
Associate Professor of Mechanical Engineering in Advanced Manufacturing Technologies
Amirkabir University of Technology
Email: amirah@aut.ac.ir

Abbas Pak
Ph.D student of Manufacturing Engineering.
School of Engineering, Tarbiat Modarres University
Email: a_pak@modares.ac.i

Alireza Shahidi
MSc and Senior Researcher in Manufacturing Engineering
Email: Alireza_shahidi@yahoo.com

Abstract

Finite element method (FEM) has been employed extensively for vibration modal analysis of piezoelectric transducers and devices. Recently, there has been a growing interest in the simulation and analysis of piezoelectric transducers by using equivalent electrical circuit models. This paper has been devoted to such purpose for an ultrasonic sandwich transducer having longitudinal vibrations for high power applications. By analytical analysis, the dimensions of the transducer components were obtained such that the resonance frequency of transducer to be 22KHz for 3KW power emission. By using a 2D finite element model, a current source was connected directly to the model. Also, equivalent electrical-circuit models were developed. Then, the models were analyzed by ANSYS and resonance, anti-resonance frequencies and also voltage, current and equivalent impedance variations were obtained. Finally, simulation and experimental results were compared.

Keywords: ultrasonic transducer, equivalent electrical circuit, Finite Element Modeling

I. INTRODUCTION

High power ultrasound is nowadays used in a wide variety of applications ranging from medical devices, ultrasonic cleaning, ultrasonic welding and machining to sono-chemistry [1]. Since Prof. Langevin developed the first sandwich ultrasonic transducer by embedding piezoelectric rings between two metallic pieces and employed the assembly for high intensity vibration, there have been great efforts in modeling and formulating such transducers [2-6]. One of the well known works is the Mason's analysis for the PZT transducers; i.e. the Equivalent Circuit Method (ECM) [7, 8]. In this method, the impedance properties of a piezoelectric transducer are presented near an isolated resonance by a lumped-parameter equivalent circuit, the simplest form of which is shown in figure 1. In this figure, two of the most widely used lumped-parameters piezoelectric converter impedance models have been shown, when thermal dissipative elements in the piezo-ceramic, matching and backing parts could be ignored.

The simulation of a piezoelectric transducer by these circuits is useful only if the circuit parameters are constant and independent of frequency. In general, the parameters are approximately independent of frequency only for narrow range of frequencies near the resonance frequency and only if the mode in question is sufficiently isolated from other modes.

The elements given in figure 1 are: C_s; static capacitance of piezo-ceramics, L_1 and C_1; equivalent motional mass and compliance elements of the transducer respectively and R_1; relates to dissipative power loss which is attributed to the joint losses (from planar friction losses between piezo-ceramics and metal parts), and to the material hysteretic-related losses (internal mechanical damping in all transducer parts). Equivalent electrical circuit models are expressed in terms of easy measurable or quantifiable parameters like resistance, capacitance, inductance, voltages and currents.

This paper presents and compares the results of electrical solution of a high power piezoelectric-transducer by four methods; using analytical relationships, using ANSYS capability for solving the proposed equivalent electrical model by the authors, employing piezoelectric transducer modeling capability on the ANSYS itself and using experimental results.

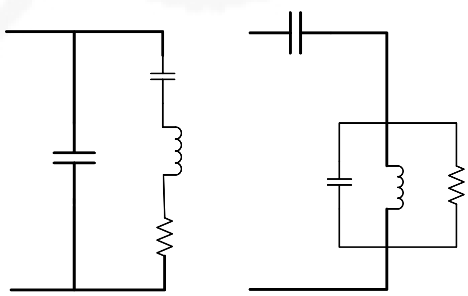

Fig. 1- Typical equivalent electrical circuits for piezoelectric transducers

In the present work, by using the analytical method, the dimensions of components of a 3KW ultrasonic transducer were determined by assuming resonance frequency of 22 KHz. Then, the finite element 2-D model of this transducer was created in ANSYS and afterwards an electrical power supply was connected directly across the piezoelectric of the model. This analysis was used to determine the values of the equivalent-circuit elements like capacitance and inductance, voltage and current variations and also to obtain resonance and anti-resonance frequencies. This is also a tool for optimization of the power supply behavior and transducer quality, knowing how to model and calculate the mechanical load, realizing optimal resonant frequency and to have a control on the out put power.

II. FEM MODELING OF THE ULTRASONIC TRANSDUCER

The analyzed transducer was composed of six PZT-4 piezo-ceramic rings, a steel cylinder-shaped back mass (St 304) and an Aluminum stepped front mass (Al 7075-T6). The bolt material was taken from steel. As the exact value of density and sound speed of the materials must be utilized in the design process, these two properties were accurately measured for backing and matching. Measurement of sound speed was made in the NDT Laboratory by using ultrasonic equipment ASCANWIN, E2.58, 2002. The time of flight (TOF) of the pulse which was transmitted and received by a single probe of 2MHz, Φ24 was measured. By knowing the thickness of the specimens, the sound speed could be obtained by a simple calculation. The material properties of the components are as shown in tables I, to V. Figures 2 and 3 show the designed transducer.

For the transducer design discussed in this paper, PZT-4 was chosen as piezoelectric material. PZT-4 is an appropriate choice for this application because it can generate high power similar to PZT-5A [10].

TABLE I
MATERIAL PROPERTIES OF ALUMINUM MATCHING [9]

Standard Code	AL 7075-T6
Measured Sound Speed (m/s)	6210
Tut (MPa)	572
Modulus of elasticity $\left(N/m^2\right)$	7.7×10^{10}
Major Poisson's ratio	0.33
Minor Poisson's ratio	0.33
Measured Density $\left(Kg/m^3\right)$	2823

TABLE II
MATERIAL PROPERTIES OF STEEL BACKING [9]

Standard Code	St 304
Measured Sound Speed (m/s)	5720
Tut (MPa)	505
Modulus of elasticity $\left(N/m^2\right)$	20.7×10^{10}
Major Poisson's ratio	0.292
Minor Poisson's ratio	0.292
Measured Density $\left(Kg/m^3\right)$	7868

TABLE III
MATERIAL PROPERTIES OF STEEL BOLT [9]

Modulus of elasticity $\left(N/m^2\right)$	20.7×10^{10}
Major Poisson's ratio	0.292
Minor Poisson's ratio	0.292
Measured Density $\left(Kg/m^3\right)$	7868

TABLE IV
MATERIAL PROPERTIES OF NICKEL ELECTRODES [9]

Modulus of elasticity $\left(N/m^2\right)$	20.7×10^{10}
Major Poisson's ratio	0.31
Minor Poisson's ratio	0.31
Density $\left(Kg/m^3\right)$	8880

Morgan Matroc Inc., a popular manufacturer of piezoelectric ceramics, lists the material properties of PZT-4 as [10]:

TABLE V
MATERIAL PROPERTIES OF PIEZOELECTRIC, PZT-4

Measured Density $\left(Kg/m^3\right)$	7640

Dielectric Relative Permittivity Matrix at Constant Strain, $\left[\varepsilon_r^S\right]$(polarization axis along Y-axis):

$$\left[\varepsilon_r^S\right]=\begin{bmatrix} 730 & 0 & 0 \\ 0 & 635 & 0 \\ 0 & 0 & 730 \end{bmatrix}$$

Piezoelectric Stress Matrix (Stress developed/electric field applied at constant strain), [e] (polarization axis along Y-axis):

$$[e]=\begin{bmatrix} 0 & -5.2 & 0 \\ 0 & 15.1 & 0 \\ 0 & -5.2 & 0 \\ 12.7 & 0 & 0 \\ 0 & 0 & 12.7 \\ 0 & 0 & 0 \end{bmatrix} C/m^2$$

Compliance Matrix [s] for PZT-4 under constant electric field, $[s^E]$ (polarization axis along Y-axis):

$$\left[s^E\right]=\begin{bmatrix} 12.3 & -5.31 & -4.05 & 0 & 0 & 0 \\ -5.31 & 15.5 & -5.31 & 0 & 0 & 0 \\ -4.05 & -5.31 & 12.3 & 0 & 0 & 0 \\ 0 & 0 & 0 & 39 & 0 & 0 \\ 0 & 0 & 0 & 0 & 39 & 0 \\ 0 & 0 & 0 & 0 & 0 & 32.7 \end{bmatrix} \times 10^{-12}\, m^2/N$$

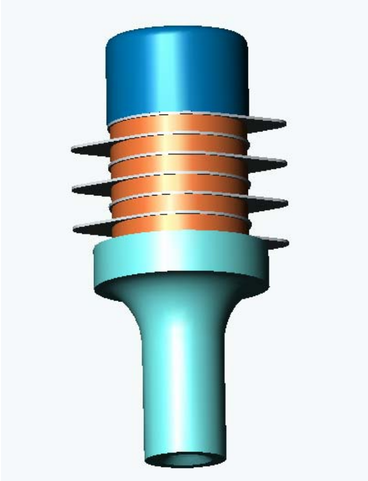

Fig.2- Modeled high power ultrasonic transducer (3KW)

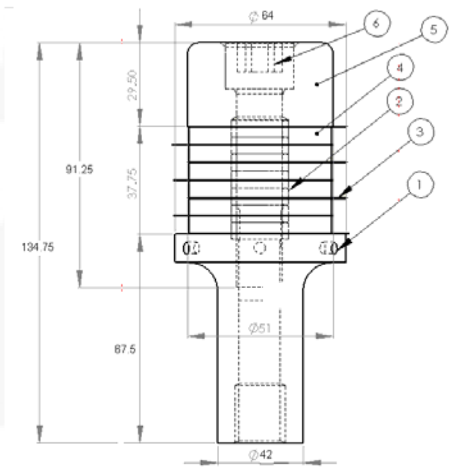

Fig.3- Dimensions of the modeled high power ultrasonic transducer (3KW)

No structural constraint was used for the modal analysis. This produces a simulation of an unrestrained transducer assembly. This state is similar to the state of physical testing where the transducer rests on the table with no restriction.

This model ignores presence of the electrically-insulating mechanically-aligning polymer (PTFE) bushes, normally used inside the ceramic disks hole around clamping bolt shank, as they are free and not stressed during the assembly. Furthermore, although transducer performance has been observed to drift slightly during operation as the ceramic pieces warm up due to losses, the temperature effects were ignored in this study.

To observe the vibration behavior through its simulation by modal analysis, the finite element method provided by commercial ANSYS was employed for 2D axi-symmetric modeling and analysis by using PLANE223 elements used for piezoelectric and PLANE13 elements used for other components. PLANE223 has a 2-D Structural-Thermal, Structural–Thermoelectric, Piezoresistive, Piezoelectric, Thermal-Electric, Thermal-Piezoelectric field capability and has eight nodes with up to four degrees of freedom per node (figure 4). PLANE13 has a 2-D magnetic, thermal, electrical, piezoelectric and structural field capability. This element is defined by four nodes with up to four degrees of freedom per node. For this modeling the element size was selected to be 1 mm.

.

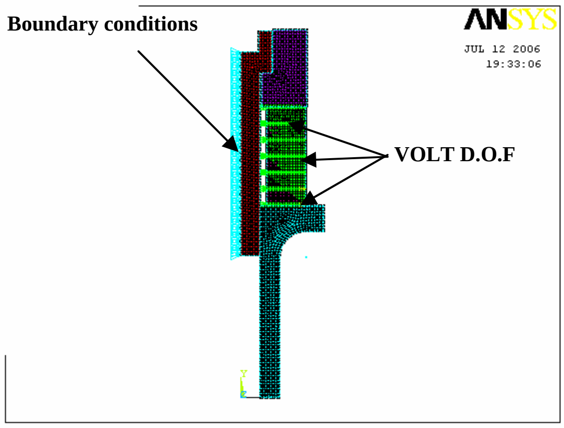

Fig. 4- 2D axi-symmetric modeling with PLANE223 elements used for piezoelectric and PLANE13 elements used for other components

III. FEM-CIRCUIT COUPLED SIMULATION

A FEM-circuit coupled piezoelectric simulation method based on electric charge balance has been described in reference [11]. In this analysis the positive faces of the piezoelectric rings are electrically connected together and also the negative faces are electrically coupled together (piezoelectric rings are electrically connected in parallel), the nodes on these faces are coupled together as equi-potential points (voltage D.O.F[1] - see figure 4). This is a good assumption as the piezoelectric pieces actually have a thin silver coating to insure excellent electrical contact.

The modeled transducer was used in static and dynamic transient simulations. Also modal and harmonic analysis were performed to understand the transducer's electromechanical behavior and to inspect its resonance frequency and its voltage and current variations [12].

A. Static analysis

The static analysis was implemented to determine the total equivalent static capacitance of the total piezoelectric rings. The piezoelectric rings were modeled with PLANE223 elements.

The negative faces (poles) of the piezoelectric rings were connected to zero voltage of common ground and a unit voltage (1V) was applied to other poles (positive faces) connection. After static analysis, the total stored electric charge on positive poles was determined by ANSYS. Then, by using equation (1) the equivalent static capacitance; C_s was calculated as:

$$C_s = \frac{Q}{V} = 1.64 \times 10^{-8} = 16.4nF \qquad (1)$$

Where Q is the total electric charge stored (C) and V is the applied voltage (V).

[1] Degree Of Freedom

Alternatively, in the static state, by using analytical relationship under constant stress (e.g. free state), the static capacitance of the piezoelectric can be calculate as ($\varepsilon^T_{r_{33}} = 1300$ [10]):

$$C = \varepsilon^T{}_{r_{33}} \varepsilon_0 . \frac{A}{\ell} =$$

$$= 1300 \times 8.85 \times 10^{-12} \times \frac{\pi \times (0.05^2 - 0.02^2)}{4 \times 0.006} = 3.16nF$$

Then for six piezoelectric rings, C_{total}:

$$C_{total} = 6 \times C = 6 \times 3.16 \times 10^{-9} = 18.975nF$$

C: Capacitance of one piezoelectric (F)

$\varepsilon^T_{r_{33}}$: Dielectric relative permittivity at constant stress (e.g. free state) along polarization axis

ε_0 : Vacuum permittivity (8.85×10^{-12} F/m)

A: Piezoelectric surface area (m^2)

l: Piezoelectric thickness (m)

As it is seen, there is a difference between the static analysis and analytical results. This difference can result from the real condition of the static analysis by ANSYS where the piezoelectric rings used in the transducer are stressed and bounded by two metal masses and an elastic clamping screw. Therefore, they are not completely free similar to analytical condition ($\varepsilon^T_{r_{33}} = 1300$) and not completely clamped ($\varepsilon^s_{r_{33}} = 635$).

B. *Transient analysis of the piezoelectric transducer and the equivalent circuits*

This is an analysis by ANSYS for a circuit in which the piezoelectric transducer is connected parallel to a resistor (R) and excited suddenly by an independent electric current source (I) as shown in figure 5. Alternatively, ANSYS analyzed an equivalent electrical circuit in which the piezoelectric transducer was approximated and replaced by the equivalent capacitor (C_s) the value of which had been determined from the static analysis of the piezoelectric by ANSYS (see figure 6). In both cases the current source and parallel resistor were identical. Transient analysis is performed for determination of the variation of the current passing through the resistor with time. There is another possibility to calculate the current variation analytically by equation 2.

$$I = I_0 (1 - e^{-t/RC}) \qquad (2)$$

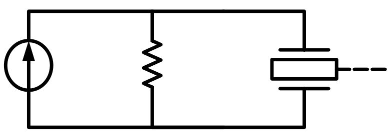

Fig 5-Piezoelectric transducer electrical circuit in the transient analysis by ANSYS

CIRCU94 elements were used to model the electrical components and PLANE223 elements were used to model the piezoelectric. CIRCU94 is a circuit element for use in piezoelectric-circuit analyses. The element has two or three nodes to define the circuit components and one or two degrees of freedom to model the circuit response. KEYOPT (1) settings and the corresponding real constants define the circuit components. Real constant input is dependent on the element circuit option used. A summary of the element options has been given in Table VI.

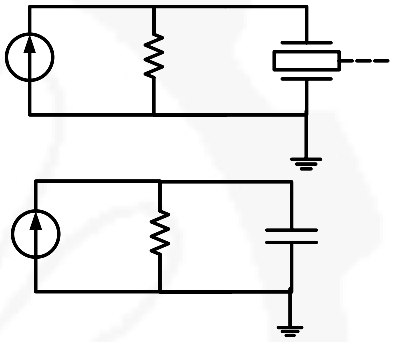

Fig 6- a) Piezoelectric transducer electrical circuit in the transient analysis by ANSYS and b) Equivalent electrical circuit in the transient analysis by ANSYS

TABLE VI -CIRCU94 ELEMENT OPTIONS [12]

Circuit Component	KEYOPT(1)	Real Constants
Resistor (R)	0	R1 = Resistance (RES)
Inductor (L)	1	R1 = Inductance (IND) R2 = Initial inductor current (ILO)
Capacitor (C)	2	R1 = Capacitance (CAP) R2 = Initial Capacitor Voltage (VCO)
Independent Current Source (I)	3	For KEYOPT(2) = 0: R1 = Amplitude (AMPL) R2 = Phase angle (PHAS)
Independent Voltage Source (V)	4	For KEYOPT(2) = 0: R1 = Amplitude (AMPL) R2 = Phase angle (PHAS)

In this analysis, real constant input for the resistance (R) was 0.0001/Cs Ohm and analysis time (t) was selected as 2RCs second. Current level for the current source (I_0) was selected 0.001 A. The variation of the current passing through the resistor in the real piezoelectric circuit and in the resistor of the equivalent electric circuit (both obtained by FEM Transient analysis) and the variation obtained by analytical solution (equation 2) are shown in figure 7.

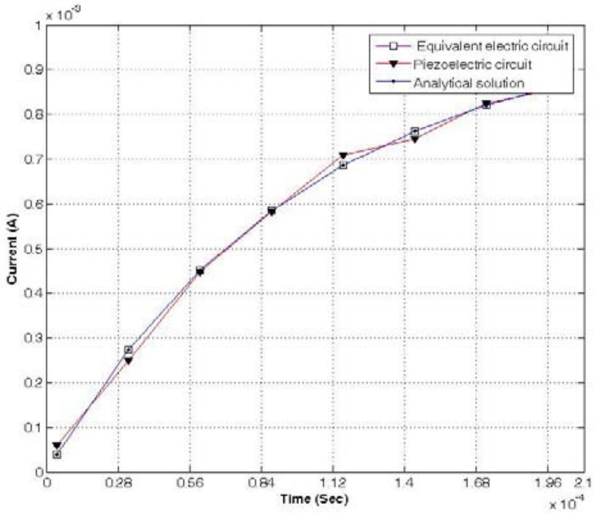

Fig. 7- The current passing through the resistor under three method of solution

C. *Modal Analysis*

Modal analysis of the piezoelectric transducer was performed to determine the resonance frequencies, f_i, and stored average electric charge, Q_i , on the positive poles in each resonance frequency (the condition resembles electric short circuit condition where the dynamic capacitive load and the dynamic inductive load cancel each other). In another attempt the piezoelectric transducer is approximated with capacitors and an inductor (C_s, C_i, and L_i) as shown in figure 8. To obtain the equivalent dynamic capacitance, $C_{i,}$ and dynamic inductance, L_i, the following equations can be used [11].

$$C_i = \frac{Q_i^2}{\omega_i^2} \tag{3}$$

$$\omega_i = 2\pi f_i \tag{4}$$

$$L_i = \frac{1}{\omega_i^2 C_i} \tag{5}$$

Q_i = Average electric charge stored on the positive poles of the piezoelectric pieces in ith piezoelectric transducer resonance frequency

ω_i = Angular frequency in ith piezoelectric transducer resonance condition

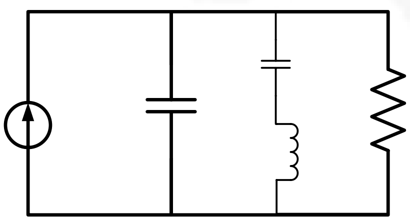

Fig 8-Equivalent electrical circuit used in modal analysis near the first piezoelectric-transducer resonance frequency

In this model R_1 element which represents dissipative power loss was not considered, as it was ignored in FEM modeling. This loss is composed of joint and friction losses between piezoelectric rings and metal parts, and internal mechanical damping in transducer's components. Results from modal analysis have been summarized in table VII.

TABLE VII-RESULTS OBTAINED FROM MODAL ANALYSIS

Mode No. (i)	Frequency (Hz)	C_i (F)	L_i (H)
1	0.42665×10^{-2}	3.15×10^{-24}	4.418×10^{26}
2	17308	3.2896×10^{-9}	0.0257
3	25000	2.25×10^{-9}	0.01795
4	29853	0.1188×10^{-9}	0.239
5	35684	0.000465×10^{-9}	42.77
6	40700	0.09615×10^{-9}	0.159
7	43218	0.000354×10^{-9}	38.275
8	43858	0.0191×10^{-9}	0.6898
9	49224	0.04642×10^{-9}	0.225

D. *Harmonic Analysis*

For harmonic analysis of the above models, it was assumed that the structure of the transducer is under no constraint. The harmonic analysis was performed over a frequency span inside which the longitudinal-mode resonance frequency was expected (0.95 to 1.1 times the frequency obtained by modal analysis). This frequency span was divided into 100 steps for determining voltage and current variations in the piezoelectric transducer circuit and in the equivalent electric circuit.

To represent the piezoelectric transducer more accurately, it would be appropriate to add branches of capacitor-inductor to the reduced order model. For example, use nine capacitor-inductor branches as shown in figure 9. The nine C_i-L_i (i = 1, 2 ... 9) branches correspond to the first nine resonance modes of the piezoelectric transducer. The equivalent static capacitance and resistance values can be adjusted to:

$$C_0 = C_s - \sum_{i=1}^{i=9} C_i \tag{6}$$

$$R = \frac{0.9}{\omega_2 C_0}$$

ω_2 = Angular frequency of the second resonance mode

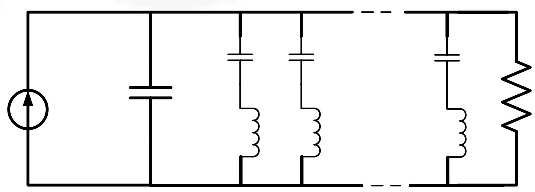

Fig. 9- Equivalent electrical circuit used in harmonic analysis near the second piezoelectric transducer resonance frequency

The voltage and current variations in the piezoelectric circuit and in the transducer equivalent electric circuit obtained from Harmonic analysis by ANSYS have been shown in figures 10 and 11.

Figure 12 shows the electrical impedance of the piezoelectric transducer circuit and also the electrical impedance of the equivalent electric circuit which was calculated by dividing voltage over current (V/I).

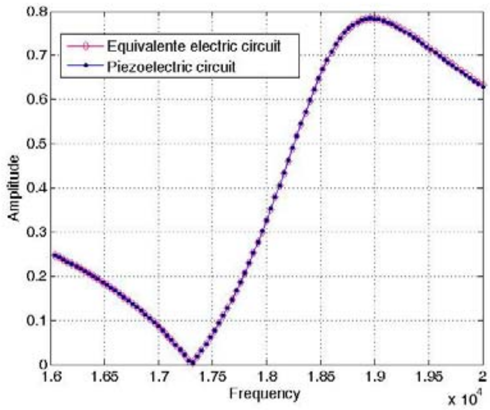

Fig. 10- The voltage across the piezoelectric transducer circuit and the equivalent electric circuit against frequency, both obtained from ANSYS harmonic analysis

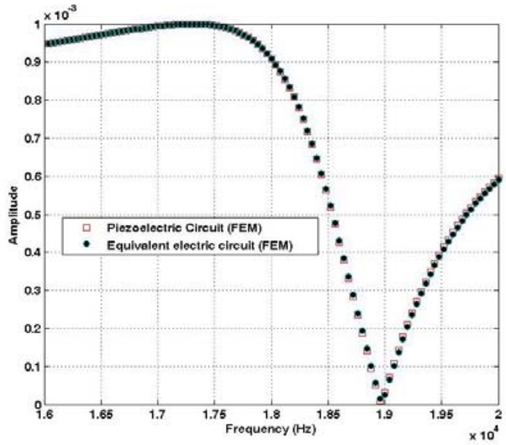

Fig. 11- Current variations in the piezoelectric transducer circuit and in the equivalent electric circuit against frequency, both obtained from ANSYS harmonic analysis

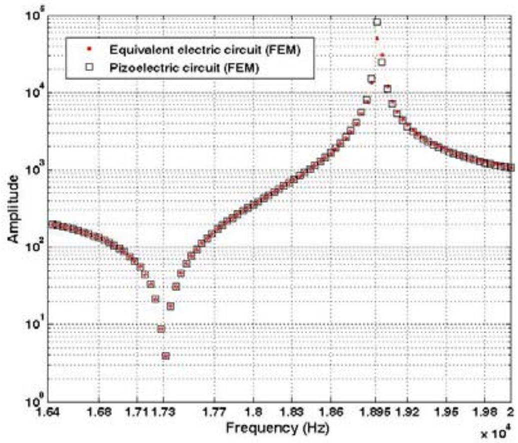

Fig. 12- Equivalent Impedance of the piezoelectric transducer circuit and equivalent impedance of the equivalent electric circuit against frequency, both obtained from ANSYS harmonic analysis

IV. TEST OF THE FABRICATED TRANSDUCER

To measure the actual resonant frequency of the designed and fabricated ultrasonic transducer a Network Analyzer of ROHDE & SCHWARZ was employed. The sweeping frequency of this device was within 9kHz-4GHz with a resolution of 10Hz. The sweeping frequency was set between 10 kHz to 30 kHz and the system was calibrated. Then, phase-versus-frequency diagram was drawn (see figure 13). Both the series and parallel frequencies are observed in the diagram. The measurement was made with the transducer under loaded and unloaded conditions. It should be noted, however, that simulation of the loading condition is greatly dependent upon the transducer application. The tests showed that, under free state, the resonance and anti-resonance frequencies were f_s=*17200Hz* and f_p=*18970Hz* respectively.

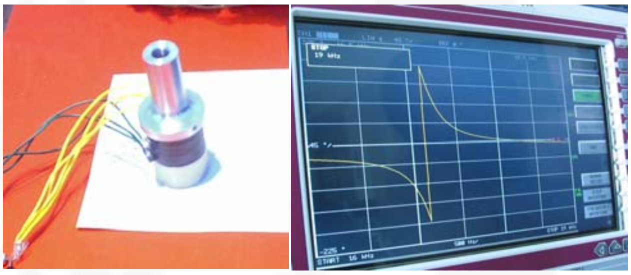

Fig 13- Fabricated transducer and the diagram of phase versus frequency generated by Network Analyzer in unloaded condition

V. COCLUSIONS

The finite element approach presented in this paper was implemented by the general-purpose finite element package ANSYS release 10. The study presented concludes:

1. FEM modeling by ANSYS proved that this software is a good tool for equivalent electrical circuit simulation of high power ultrasonic piezoelectric-transducers and also it shows an good conformity with the piezoelectric impedance modeling.

2. As shown in figures 7, 10, 11 and 12 there is a good conformity between the results obtained from the piezoelectric transducer electrical circuit modeling and the equivalent electric circuit simulations. These also show a very close resonance and anti-resonance frequencies with the network analyzer test results.

3. Figure 7 shows that, under sudden connection of a current source to the models, the current passing through the parallel resistor under analytical and two FEM modeling methods have a very close conformity.

4. The FEM model is a computer approximation of an actual structure. The error of this approximation will depend on the consideration of all the system

components, their accurate properties, appropriate selection of the elements and refinement of the model.

5. The influence of an external acoustic load on the transducer can be modeled by adding a resistance, R, to the equivalent electric circuit. However, it is very difficult to model the effect of an external load on ultrasonic transducer.

NOMENCLATURE

A	Piezoelectric surface area	m^2
C_0	Adjusted dynamic capacitance	F
C_i	Dynamic capacitance	F
C_s	Equivalent static capacitance	F
e	Piezoelectric Stress Matrix	C/m^2
f_i	Resonance frequency	Hz
f_p	Anti-resonance frequency	Hz
I	Current	A
I_0	Maximum current	A
l	Piezoelectric thickness	m
L_i	Dynamic inductance	H
R	Resistance	Ω
s^E	Compliance Matrix under constant electric field	m^2/N
t	Analysis time	Sec
V	Voltage	V
Q_i	Average electric charge of the piezoelectric pieces in ith piezoelectric transducer resonance frequency	C
ω_i	Angular frequency in ith piezoelectric transducer resonance condition	Rad/Sec
$\varepsilon^T_{r_{33}}$	Dielectric Relative Permittivity Matrix at Constant Strain	-
$\varepsilon^s_{r_{33}}$	Dielectric Relative Permittivity Matrix at Constant Strain	-
ε_0	Vacuum permittivity (F/m)	F/m

ACKNOWLEDGMENT

This work was funded by Persian Keyan Technologies Co. Thanks should also be given to Electrical Engineering Faculty of Amirkabir University of Technology. Authors express their sincere appreciation to Dr. Prokic and his colleagues at MPInterconsulting for providing invaluable guides and helpful comments.

REFERENCES

[1] R. Frederick, 1965, "*Ultrasonic Engineering*", John Wiely & Sons, Inc., New York.
[2] P. Langevin, French Patent No. 502913 (29.51920); 505703 (5.8.1920); 575435 (30.7.1924).
[3] W.P. Mason, 1942, "*Electromechanical Transducers and Wave Filters*", D. Van Nostrand, New York.
[4] R. Krimholtz, D.A. Leedom, G.L. Mattaei, 1970, "*New equivalent circuits for elementary piezoelectric transducer*" Electron. Lett, 398–399.
[5] M. Redwood, 1964, "*Experiments with the electrical analog of a piezoelectric transducer*", J. Acoust. Soc. Am. 36 (10) 1872–1880.
[6] Kagawa, Y., Yamabuchi, T., Mar 1979, "*Finite Element Simulation of a Composite Piezoelectric Ultrasonic Transducer*" IEEE Transactions on Sonics and Ultrasonics, Volume 26, Issue 2, Page(s):81 – 87.
[7] W. P. Mason "*Electromechanical Transducers and Wave Filters*", Van Nostrand, Princeton, NJ, (1948)
[8] W. P. Mason "*Piezoelectric Crystals and their Applications to Ultrasonic*", Van Nostrand-Reinhold, Princeton, NJ (1950).
[9] http://www. matweb .com
[10] Morgan Matroc Inc., 2006, "*Piezoelectric Technology Data for Designers*", Morgan Matroc Inc., Electro Ceramics Division.
[11] Jian S. Wang and Dale F. Ostergaard, 1999, "*A Finite Element-Electric Circuit Coupled Simulation Method for Piezoelectric Transducer*" IEEE Ultrasonic Symposium, 1105-1108.
[12] ANSYS Instructions, Release 10, ANSYS Inc., July 2005.